S-nitrosated polypropylene sulfide nanoparticles for thiol-dependent transnitrosation and toxicity against adult female filarial worms

Alex Schudel,

School of Materials Science and Engineering and Parker H. Petit Institute for Bioengineering and Bioscience, Georgia Institute of Technology, 315 Ferst Dr NW, Atlanta, GA 30332, USA

Timothy Kassis,

School of Electrical and Computer Engineering and Parker H. Petit Institute for Bioengineering and Bioscience, Georgia Institute of Technology, 315 Ferst Dr NW, Atlanta, GA 30332, USA

J. Brandon Dixon, and

George W. Woodruff School of Mechanical Engineering and Parker H. Petit Institute for Bioengineering and Bioscience, Georgia Institute of Technology; Wallace H. Coulter Department of Biomedical Engineering, Georgia Institute of Technology and Emory University, 315 Ferst Dr NW, Atlanta, GA 30332, USA
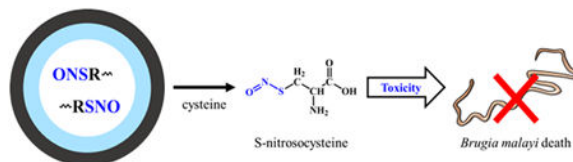
Susan N. Thomas

George W. Woodruff School of Mechanical Engineering and Parker H. Petit Institute for Bioengineering and Bioscience, Georgia Institute of Technology; Wallace H. Coulter Department of Biomedical Engineering, Georgia Institute of Technology and Emory University; Winship Cancer Institute of Emory University, 315 Ferst Dr NW, Atlanta, GA 30332, USA

Susan N. Thomas: susan.thomas@gatech.edu

Abstract

A synthetic polymer nanoparticle formulation utilizing the physiological nitrosothiol chemistry for nitric oxide delivery. Toxicity of SNO-NP against adult female *Brugia malayi* worms, which are responsible for lymphatic filariasis, is dependent on nitric oxide release through transnitrosation as S-nitrosocysteine, a potent endogenous nitric oxide donor.

Graphical abstract

Correspondence to: Susan N. Thomas, susan.thomas@gatech.edu.

Keywords

B. malayi; nanoparticle; nitric oxide; nitrosothiol; NO donor

Nitric oxide (NO) mediates its effects through its chemistry in a variety of physiological signaling processes including vasodilation,[1] inhibition of platelet aggregation,[2] and cytotoxicity[3] in a manner analogous to phosphorylation.[4] NO is highly diffusive, but due to its chemical reactivity is purported to have an extremely short half-life on the order of 5-10 seconds.[5] Controlled delivery and release strategies for NO are thus highly attractive for a range of therapeutic applications,[6] but challenging to achieve within deep tissue targets.[7]

To enable NO's physiological effects to be exerted over much farther distances than its reactivity-limited diffusion distance would permit, NO *in situ* can form reversible adducts with endogenous nucleophiles[8] or convert to its more stable oxidized forms, nitrite (NO_2^-) and nitrate,[9] all of which can revert to NO under certain physiological conditions.[9, 10] Endogenous nitrosothiols (R-SNO), which include S-nitrosocysteine (SNO-CYS), S-nitroso-albumin, and S-nitrosoglutathione, represent a major class of NO adducts that facilitate NO's transport *in vivo*.[11] R-SNO are formed on free thiols either through reactions with nitrosating agents[12] or by transnitrosation (i.e. by transfer of NO from other nitrosothiols)[13, 14] giving R-SNO the ability to be formed under a wide range of (patho)physiological conditions.[15] Therefore, in addition to NO_2^- and nitrate, which have previously been explored for therapeutic delivery as prodrugs,[16] R-SNO represent an attractive and physiological NO chemistry that has been exploited to harness both native NO signaling and transport activity in biological systems.[17]

Brugia malayi, one of three filarial worms responsible for lymphatic filariasis, are transmitted through a mosquito's saliva, injected into a host's dermis, where they make their way to the lymphatics, grow and multiply, and can eventually cause several chronic diseases including elephantiasis.[18] There are an estimated 120 million people, most of whom reside in the developing world, who harbor these parasites with another 1 billion people identified as at risk for infection.[19] While there are several treatment options available to remove the microfilaria progeny that spread the disease, there are no lymphatic-localized therapies that target the adult worms in the lymphatics where they reside. Hence, people currently infected face few treatment options.[19]

NO has been implicated as an effector cytotoxic molecule in the immune response to a variety of pathogenic parasites.[18, 20, 21] Previous work has shown that *B. malayi* are susceptible to exogenously delivered NO[22] and demonstrated potential for physiological R-SNO, SNO-CYS[23] and S-nitrosoglutathione,[24] to mediate damage to several types of parasites. Due to their small size, however, commercially available NO donors and physiological R-SNO have low potential after injection to accumulate within lymphatic vessels[25, 26] where these parasites reside, curbing their utility as anti-filarial therapeutic agents. Whereas small molecules <5 nm in hydrodynamic size are freely blood permeable and are thus rapidly cleared into the systemic circulation[25], drug targeting to lymphatics is significantly enhanced for nanoscale drug delivery systems ∼30 nm in hydrodynamic

size[25] and NO formulation approaches improve both donor circulation times[27] and NO bioactivity.[28] An NO-encapsulating nanoformulation could therefore facilitate the targeted, controlled, and efficient delivery of NO to eradicate filarial parasites resident within lymphatic tissues.

Herein, we report the synthesis and modification of thiolated nanoparticles (NP) with NO in order to harness the physiological nitrosothiol chemistry for NO delivery and bioactivity using a synthetic polymer system. These NO-containing nanoparticles (SNO-NP) stably encapsulate high levels of NO and facilitate its controlled release. In particular, we demonstrate that the bioactive form of released NO from SNO-NP, either NO_2^- or SNO-CYS, depends on the ratio of free cysteine (CYS), a common endogenous low molecular weight thiol important in transnitrosation reactions,[15] to SNO-NP. Furthermore, the cytotoxic activity of SNO-NP against *B. malayi* adult female filarial worms, for which there is no existing treatment, is accelerated in the presence of CYS due to the formation of SNO-CYS. Since these synthetic NP have well-documented lymphatic targeting activity after intradermal injection,[30] these results provide a strong rationale for therapeutic use of SNO-NP in eradication of *B. malayi* that reside intralymphatically *in vivo* and for other deep tissue NO delivery applications.

SNO-NP were formed by *S*-nitrosation of synthetic thiolated NP synthesized by emulsion polymerization[31] (Figure 1a). Amphiphilic block copolymer Pluronics, including F127 (PF127) explored here as well as F68,[32] self-assemble in water to form micelles, which are able to make an emulsion with propylene sulfide and, in the presence of a deprotected thiolated initiator, activate living anionic polymerization within the micelle core. As the concentration of initiator was varied, different degrees of polymerization of poly(propylene sulfide) were achieved (Figures S1-4). This resulted in an increasing concentration of free thiols (SH) (Figure 1b) as well as ratio of SH to disulfide (Figure S5) at the completion of polymerization after solution oxidation with increasing concentration of added initiator with little to no effect on NP size (Figure 1c). Dialyzed NP were subsequently *S*-nitrosated by introduction of acidified nitrite, enabling formation of NO *S*-nitroso adducts (SNO) with the NP core free thiols. With increasing concentration of NP SH there was a proportional increase in SNO concentration created as measured by a modified method of Saville[14], indicating efficient S-nitroso adduct formation (Figure 1d) that was determined to be >90% for all starting NP free thiol concentrations. This occurred with no change in NP size (Figure 1c), and resulted in up to an estimated 2000 SNO per NP (Figure 1d). To confirm SNO adduct formation within NP, SNO-NP were analyzed via UV-VIS absorbance. SNO-NP exhibited the characteristic absorbance wavelength of primary thiol *S*-nitroso adducts at approximately 340 nm,[29] that increased with concentration (Figure 1e) giving a molar extinction coefficient of 540 M^{-1} cm^{-1} (Figure 1e, inset) consistent with previously reported R-SNO.[13] Furthermore, the SNO signal co-eluted with that of the thiolated NP during column chromatography (Figure 1f), demonstrating the stability of the SNO adduct. Additionally, over the course of dialysis at room temperature against water in a membrane with a 100,000 molecular weight cut off, SNO signal did not decline appreciably while free NO_2^- from the S-nitrosation process was effectively removed as the pH of SNO-NP was brought to physiological levels (Figure 1g).

We next explored the release of NO from SNO-NP under physiological conditions. In complete serum-containing media at 37°C, decay of SNO signal from 1 mM of SNO-NP over 100 hr was comparable to that of 1mM of *S*-nitroso-N-acetyl penicillamine (SNAP), a commercially available synthetic small molecule NO donor[10] that is similar in size and structure to some endogenous R-SNO, which has been extensively used to study a wide variety of NO-regulated processes including inflammation,[33] vasodilation,[34] and inhibition of platelet aggregation.[10] The rate of NO release from SNO-NP was not influenced by the degree of PS polymerization (Figure S6). At 6 and 24 hr post incubation, however, SNO-NP exhibited faster release (32% and 70%, respectively) of SNO relative to SNAP (7% and 50%) (Figure 2a). In distinct contrast to SNAP, SNO-NP also resulted in the significant accumulation over time of NO_2^- (Figure 2a), likely resulting from preferential reaction with oxygen due to its increased concentration within the hydrophobic NP core, in which oxygen is more soluble than aqueous media.[35] SNAP, on the other hand, being a small molecule NO donor that releases NO directly into a less oxygen dense environment[8] that may have potential for interactions with serum species,[36] results in no NO_2^- accumulation.

We next evaluated whether SNO-NP could donate NO to physiological thiols through transnitrosation.[13] In complete medium, the free thiol concentration was found to be <0.025 mM as measured by Ellman's assay. To probe how the presence of free thiols may drive transnitrosation, we added CYS and monitored SNO decay from SNO-NP and the formation of NO_2^- over time (Figure 2b-c). CYS was mixed with 1 mM of SNO-NP at the following ratios of CYS:SNO-NP (i.e., SH from CYS to SNO from SNO-NP): 0:1, 0.1:1, 1:1, and 10:1. CYS to SNO-NP ratios of 1:1 and 10:1 accelerated the decay of SNO signal from SNO-NP relative to low and zero CYS ratios (Figure 2b). However, an increase in SNO signal that was not statistically significant was observed at long times after co-incubation for the highest ratio tested (10:1, Figure 2b), suggesting long lived SNO species under conditions of excess CYS. Furthermore, whereas low CYS to SNO-NP ratios (0.1:1, 1:1) resulted in the appreciable accumulation of NO_2^- in a manner analogous to NO release by SNO-NP with no added CYS, a 10:1 ratio of CYS to SNO-NP did not (Figure 2c). This data suggests that under conditions of low versus high CYS, NO is released from SNO-NP by either of two distinct pathways: to NO_2^- in the case of low or no free thiols or to R-SNO via transnitrosation in the case of high thiol concentration (Figure 2d).

To test this hypothesis, the extent of transnitrosation as determined by the formation of SNO-CYS after co-incubation of 1 mM of SNO-NP with varying ratios of CYS was determined. Since the Saville assay could not discriminate between SNO retained by SNO-NP versus that from newly created SNO-CYS via transnitrosation, the two SNO species were separated using size exclusion column chromatography after prescribed times of co-incubation. This technique was able to detect the ratio of remaining SNO amongst the two species, SNO-NP and SNO-CYS, by comparing the collected fractions to those previously obtained for the individual species (Figure 2e). By virtue of their larger size, NP eluted in early fractions, whereas small CYS eluted in later fractions as verified by Ellman's assay and iodine staining.[30] We found that SNO-CYS constituted a larger percent of remaining SNO at late times for all CYS to SNO-NP ratios tested, but only represented a significant portion

of the remaining SNO for 10:1 CYS:SNO-NP (Figure 2f). In terms of absolute amount, this corresponded with an appreciable increase in SNO-CYS concentration for only the 10:1 CYS to SNO-NP (Figure 2g). The extent of transnitrosation by SNO-NP was not appreciably affected by degree of PS polymerization (Figure S7).

To demonstrate SNO-NP function as an anti-parasitic agent, we devised a setup in which adult female worms were individually incubated in wells containing complete medium and quantified motility over 96 hours. We have previously used a similar experimental configuration to monitor worm motility and health over time as well as evaluate worm responses to anti-parasitic agents.[37] Worm motility in response to treatment normalized to pre-treatment was then plotted over time. Concentrations of NO treatment groups ranged from 1-2 mM.

We found that the motility of SNAP-treated worms decreased quickly upon co-incubation with SNAP, while control N-acetyl penicilamine (NAP)-treated worms showed no reduction (Figure 3a). Treatment with SNO-NP but not NP alone also resulted in a reduction of worm motility though the response was much delayed relative to SNAP (Figure 3a). However, the death curve (Figure 3b) and the time until death (Figure 3e), defined as when motility dropped below 10% of baseline, were similar for both SNAP and SNO-NP treated worms. We hypothesized that this discrepancy in effect on motility but not time until death may result from SNAP but not SNO-NP penetration into the worms in order to mediate its effects. This idea is supported by findings that the worm's cuticle, the highly cross-linked collagenous structure lining the worm's limiting membrane,[38] is impermeable to large antibody and complement complexes,[39] but not to small molecules such as glucose or amino acids, thus making it impermeable to the SNO-NP.[40] Furthermore, it has been previously hypothesized that endogenous R-SNO, which are similar in molecular weight and hydrodynamic size to SNAP, mediate anti-parasitic effects through their uptake by worms as the result of their similarity to natural analogues[23] and by S-nitrosating key proteins[41] such as cysteine proteases.[21, 42] To test this hypothesis, worms were incubated with SNO-NP in the presence of 0:1. 0.1:1, 1:1, and 10:1 CYS:SNO-NP. Treatment with CYS alone did not have a negative effect on worm motility and did not result in any worm death. When worms were incubated with SNO-NP at a 0.1:1 ratio with CYS, a similar effect on worm motility as that of SNO-NP alone (Figure 3c) was found. However, when CYS was present at a 1:1 ratio, the reduction in motility closely matched that induced by SNAP (Figure 3c). Intriguingly, when CYS was present at the ratio 10:1 with SNO-NP, the reduction in motility induced by treatment was almost immediate (Figure 3c) and resulted in a dramatically faster time until death than that of SNAP (Figure 3e). Worm treatment with SNO-NP in combination with increasing amounts of CYS up to a ratio of 1:1 resulted in the same death curve as SNAP relative to PBS (Figure 3d). However, treatment with SNO-NP in combination with CYS at the highest ratio tested (10:1) resulted in death curves that were accelerated relative to those induced by treatment with other CYS:SNO-NP ratios and SNAP (Figure 3d). This significant difference, as exemplified by the rapid time until death of 10:1 CYS:SNO-NP (Figure 3e), may be a result of the higher amount of total SNO-CYS created when CYS is added at a high ratio relative to SNO-NP (Figure 3f). It should be noted that though cysteine is present in the lymph at ∼100 uM,[43] SNO-NP undergo significant dilution following intradermal administration, accumulating within lymph in

draining lymph nodes at a ~30-100-fold lower concentration relative to that administered in the dermis.[30] Hence if the dose used *in vitro* here was administrated intradermally, SNO-NP would still result in CYS:SNO-NP ratios >3-10. Additionally, SNO-CYS (187 Da), which is approximately the same size as SNAP (220 Da), may kill the worms faster either because it is absorbed more quickly than SNAP or because it is better at mediating the effects of the NO it carries. In addition to their higher potential for lymphatic targeting relative to SNAP, these results highlight the potential for SNO-NP to effectively treat parasites through its unique NO-releasing mechanisms.

In conclusion, we have demonstrated the synthesis and characterization of SNO-NP for the delivery of NO reservoirs NO_2^- and R-SNO. We demonstrate that SNO-NP release SNO through either the formation of NO_2^- or by transnitrosation. Furthermore, we establish anti-parasitic activity of SNO-NP corresponding with the extent of R-SNO formation determined by the relative ratio of CYS to SNO-NP (Figure 3f). Implementing a synthetic polymer nanoformulation to deliver high levels of per NP NO via the physiological *S*-nitrosothiol chemistry represents an innovative approach to achieve therapeutic delivery of NO. Given the unique and previously reported lymphatic targeting activity of these NP, this represents a novel formulation for the delivery of NO in the elimination of adult female filarial worms.

Experimental Section

Synthesis and Characterization of SNO-NP

NP were synthesized as previously described.[30, 31, 44] Briefly, 500 mg of Pluronic F127 (Sigma-Aldrich, St. Louis, MO, USA, P2443) was added to 10 mL of degassed Milli-Q water, allowed to dissolve for 30 min with stirring, and was again degassed. To this solution, 400 μL of propylene sulfide (Sigma-Aldrich, P53209) was added under Argon and stirred for 30 min. Initiator weighing 7.8, 14.4, 28.8, or 43.4 mg (1.9, 3.7, 7.4, and 11 mM, respectively) was reacted with 322 μL of sodium methoxide (Sigma-Aldrich, 156256) and then added under Argon. 1,8-Diazabicyclo[5.4.0]undec-7-ene (DBU) (Sigma-Aldrich, 139009) was added under Argon to the solution 15 min later and the entire reaction stirred for 24 hr. The solution was subsequently exposed to air for two hr and dialyzed for three d against 4×5 L of Milli-Q water using 100,000 Da molecular weight cut off cellulose membrane dialysis tubing (Spectrum Lab., Rancho Dominguez, CA, USA, 131414). NP size was measured by dynamic light scattering and a small volume was lyophilized to obtain the total NP weight concentration. ^1H NMR (400 MHz, $CDCl_3$) was used to calculate the weight percent of Pluronic F127, poly(propylene sulfide), and initiator in the NP.[31] Ellman's assay (Thermo Scientific, Rockford, IL, USA, 22582) was used to determine the concentration of NP free thiols. Thiolated NP were *S*-nitrosated by reacting equal volumes of NP with sodium nitrite (Sigma Aldrich, 237213) solution in strong acid. Unreacted free acidified nitrite was capped with addition of ammonium sulfamate (Sigma Aldrich, 228745). SNO-NP were further dialyzed before use in transnitrosation and *B. malayi* experiments.

Determination of SNO and NO_2^- Concentration using Modified Saville and Griess Assays

Acidified nitrite solution was prepared by mixing equal volumes of 2N HCL with sodium nitrite solution (aqueous). Sulfanilamide (Sigma-Aldrich, S9251) solution was prepared by

dissolving 34 mg sulfanilamide in 1 mL of 0.4N HCL. Mercuric chloride (Sigma-Aldrich, 215465) solution was prepared by dissolving 10 mg of mercuric chloride in 1 mL of water. 5.4 mM N-(1-Naphthyl)ethylenediamine dihydrochloride (Sigma-Aldrich, 222488) solution was prepared in 0.4N HCL. In reactions where excess acidified nitrite was removed, an 8-fold molar excess of ammonium sulfamate was added to the solution. The Saville assay,[45] which measures *S*-nitrosothiol concentration, was performed by mixing 70 μL of the *S*-nitrosated thiol solution with 100 μL of Solution A (1 part mercuric chloride solution, 4 parts sulfanilamide solution) or 100 μL of Solution B (1 part water, 4 parts sulfanilamide solution) and then mixing these solutions with 80 μL of 5.4 mM N-(1-Naphthyl)ethylenediamine dihydrochloride solution. The Griess assay, which measures free NO_2^-, is the same as the Saville, except without the addition of Solution A. For both assays, after 10 min incubation at room temperature, the absorbance was read at 540 nm and the difference between Solution A and Solution B represents the *S*-nitrosothiol signal. *S*-nitrosothiol and free NO_2^- concentrations were calculated from a standard curve of *S*-nitrosoglutathione.[46]

Degradation and Transnitrosation Studies

SNO-NP were prepared by the standard *S*-nitrosation procedure described above. SNO-NP were then dialyzed with 100,000 Da molecular weight cut off cellulose membrane dialysis tubing against 5L of Milli-Q water overnight. Following dialysis, SNO-NP were brought to pH 7.4 using 10× PBS without calcium and magnesium and diluted to 1-2 mM NO concentration in complete medium. SNAP solutions were made in PBS, pH to 7.4, and diluted to 1-2 mM NO concentration in complete medium. SNO-NP in complete medium were mixed with CYS to 0.1, 1, and 10× the SNO-NP concentration. Solutions were incubated in closed vessels at 37°C and nitrite and SNO concentrations monitored over 100 hr. Transnitrosation studies were conducted as described above except SNO-NP were incubated in the presence of varying amounts of CYS for 45 min, 365 min, and 1460 min at 37 °C, after which 250 μL of the solution was fractionated on a 1 cm × 30 cm Sepharose CL-6B (GE Healthcare, Pittsburg, PA, USA, 17-0160-01) column. Eluted fractions were analyzed for NO_2^- and SNO using the Griess assay and Saville assay, respectively.

Brugia Malayi Motility and Death Studies

Freshly isolated adult female *B. malayi* parasites were obtained from the National Institutes of Health Filarial Research Resource (FR3)[47] at the University of Georgia (Athens, GA, USA). Upon receipt, worms were washed and resuspended in 50 mL of complete medium (Endothelial Basal Medium (Lonza, New York, USA) supplemented with 20% FBS (Atlanta Biologicals, Lawrenceville, GA, USA), 1% Glutamax, 1% Penicillin-Streptomycin-Amphotericin (Gibco, New York, NY, USA), 25 mg/mL cyclic-AMP and 1 mg/mL hydrocortisone acetate (both from Sigma Aldrich)). The worms were then maintained at 37°C in a 5% CO_2 incubator for at least 18 hr prior to experimentation. Individual worms were subsequently plated in 2.5 mL of complete medium in a 24-well culture plate pre-incubated at 37°C in a 5% CO_2 for 1 hr prior to the addition of worms. All treatment solutions were prepared the day of the experiment, except SNO-NP, which were *S*-nitrosated and dialyzed the prior evening. All treatment solutions were prepared in 1× PBS without calcium and magnesium at a pH of 7.4. 500 μL of each treatment was added to the worms in

replicates of four. Following the addition of treatments, the worms were incubated and 5 s video segments at 10 min intervals were recorded using a custom imaging hardware assembled and maintained within the incubator. Worm motility was quantified using a Lucas-Kanade optical flow algorithm implemented in LabVIEW (National Instruments, Austin, TX). The velocity vectors obtained between two subsequent frames were summed for an entire worm-containing well and then averaged over the length of the video segment giving us the motility metric. Worm death was defined when the motility metric (normalized to pre-treatment baseline) fell and remained below 10% of its normalized value. The 10% threshold was used after it was determined that below that the algorithm was quantifying noisy pixels due to vibrations in the incubator. Data representative of individual treatment groups run in quadruplets in two to five independently run experiments.

Statistical Analysis

Data is expressed as mean ± standard deviation. Statistical analysis was carried out using Prism 6 (GraphPad Software Inc. La Jolla, CA, USA). Death curves were analyzed using a Log-rank (Mantel-Cox) test for significance. Time until death was analyzed using an ordinary unpaired one-way analysis of variance (ANOVA) with Tukey multiple comparison correction. Statistical significance was defined as and represented by $p \le 0.05$ (*), $p \le 0.01$ (**) and $p \le 0.001$ (*** and §§§).

Supplementary Material

Refer to Web version on PubMed Central for supplementary material.

Acknowledgments

References

1. Ignarro LJ, Buga GM, Wood KS, Byrns RE, Chaudhuri G. Proc Natl Acad Sci U S A. 1987; 84:9265. [PubMed: 2827174]

2. Yao SK, Ober JC, Krishnaswami A, Ferguson JJ, Anderson HV, Golino P, Buja LM, Willerson JT. Circulation. 1992; 86:1302. [PubMed: 1394936]

3. Wink DA, Mitchell JB. Free Radical Biol Med. 1998; 25:434. [PubMed: 9741580]

4. Martinez-Ruiz A, Lamas S. Cardiovasc Res. 2004; 62:43. [PubMed: 15023551]

5. Ignarro LJ. Annu Rev Pharmacol Toxicol. 1990; 30:535. [PubMed: 2188578]

6. a) Cayatte AJ, Palacino JJ, Horten K, Cohen RA. Atertioscler, Thromb, Vasc Biol. 1994; 14:753.b) Mueller AR, Platz KP, Langrehr JM, Hoffman RA, Nussler AK, Nalesnik M, Billiar TR, Schraut WH. Transplantation. 1994; 58:1309. [PubMed: 7809922] c) Zhang F, Iadecola C. J Cereb Blood Flow Metab. 1994; 14:574. [PubMed: 8014203]

7. Kerwin JF, Lancaster JR, Feldman PL. J Med Chem. 1995; 38:4343. [PubMed: 7473563]

8. Hughes MN. Methods Enzymol. 2008; 436:3. [PubMed: 18237624]

9. Lundberg JO, Weitzberg E, Gladwin MT. Nat Rev Drug Discovery. 2008; 7:156. [PubMed: 18167491]

10. Askew SC, Butler AR, Flitney FW, Kemp GD, Megson IL. Bioorg Med Chem. 1995; 3:1. [PubMed: 8612040]

11. Orie NN, Vallance P, Jones DP, Moore KP. Am J Physiol: Heart and Circ Physiol. 2005; 289:H916. [PubMed: 15821033]

12. a) Goldstein S, Czapski G. J Am Chem Soc. 1996; 118:3419.b) Keshive M, Singh S, Wishnok JS, Tannenbaum SR, Deen WM. Chem Res Toxicol. 1996; 9:988. [PubMed: 8870986]

13. Meyer DJ, Kramer H, Ozer N, Coles B, Ketterer B. FEBS Lett. 1994; 345:177. [PubMed: 8200453]

14. Arnelle DR, Stamler JS. Arch Biochem Biophys. 1995; 318:279. [PubMed: 7733655]

15. Zhang Y, Hogg N. Free Radical Biol Med. 2005; 38:831. [PubMed: 15749378]

16. Mülsch A, Bara A, Mordvintcev P, Vanin A, Busse R. Br J Pharmacol. 1995; 116:2743. [PubMed: 8590999]

17. Miller MR, Megson IL. Br J Pharmacol. 2007; 151:305. [PubMed: 17401442]

18. Brunet LR. Int Immunopharmacol. 2001; 1:1457. [PubMed: 11515811]

19. Bockarie MJ, Taylor MJ, Gyapong JO. Expert Rev Anti-Infe. 2009; 7:595.

20. Rajan TV, Porte P, Yates JA, Keefer L, Shultz LD. Infect Immun. 1996; 64:3351. [PubMed: 8757874]

21. Ascenzi P, Bocedi A, Gradoni L. IUBMB life. 2003; 55:573. [PubMed: 14711001]

22. Thomas GR, McCrossan M, Selkirk ME. Infect Immun. 1997; 65:2732. [PubMed: 9199443]

23. Rockett KA, Awburn MM, Cowden WB, Clark IA. Infect Immun. 1991; 59:3280. [PubMed: 1879941]

24. Costa IS, de Souza GF, de Oliveira MG, Abrahamsohn Ide A. J Antimicrob Chemoth. 2013; 68:2561.

25. Thomas SN, Schudel A. Curr Opin Chem Eng. 2015; 7:65. [PubMed: 25745594]

26. a) Porter CJ. Crit Rev Ther Drug. 1997; 14:333.b) Bergqvist L, Strand SE, Persson BRR. Semin Nucl Med. 1983; 13:9. [PubMed: 6220471] c) Oussoren C, Zuidema J, Crommelin DJA, Storm G. Biochimica et Biophysica Acta - Biomembranes. 1997; 1328:261.

27. Swartz MA. Adv Drug Del Rev. 2001; 50:3.

28. Katsumi H, Nishikawa M, Yamashita F, Hashida M. J Pharmacol Exp Ther. 2005; 314:1117. [PubMed: 15901798]

29. Stasko NA, Fischer TH, Schoenfisch MH. Biomacromolecules. 2008; 9:834. [PubMed: 18247567]

30. Thomas SN, Vokali E, Lund AW, Hubbell JA, Swartz MA. Biomaterials. 2014; 35:814. [PubMed: 24144906]

31. van der Vlies AJ, O'Neil CP, Hasegawa U, Hammond N, Hubbell JA. Bioconjugate Chem. 2010; 21:653.

32. Rehor A, Tirelli N, Hubbell JA. Macromolecules. 2002; 35:8688.

33. Fernandes D, Da Silva-Santos JE, Assreuy J. Inflamm Res. 2002; 51:377. [PubMed: 12234054]

34. Bryan S, Alexander-Lindo R, Dasgupta T. Open Access Animal Physiol. 2011

35. Liu X, Miller MJ, Joshi MS, Thomas DD, Lancaster JR Jr. Proc Natl Acad Sci U S A. 1998; 95:2175. [PubMed: 9482858]

36. Ignarro LJ, Fukuto JM, Griscavage JM, Rogers NE, Byrns RE. Proc Natl Acad Sci U S A. 1993; 90:8103. [PubMed: 7690141]

37. a) Kassis T, Skelton HM, Lu IM, Moorhead AR, Dixon JB. PLoS Neglect Trop D. 2014; 8:e3305.b) Marcellino C, Gut J, Lim KC, Singh R, McKerrow J, Sakanari J. PLoS Neglect Trop D. 2012; 6:e1494.

38. Smith VP, Selkirk ME, Gounaris K. Mol Biochem Parasit. 1996; 78:105.

39. Selkirk ME, Blaxter ML. Acta Trop. 1990; 47:373. [PubMed: 1978537]

40. Howells RE, Chen SN. Exp Parasitol. 1981; 51:42. [PubMed: 7461090]

41. Hertz R, Ben Lulu S, Shahi P, Trebicz-Geffen M, Benhar M, Ankri S. PLoS ONE. 2014; 9:e91518. [PubMed: 24626316]

42. Siman-Tov R, Ankri S. Parasitol Res. 2003; 89:146. [PubMed: 12489015]

43. Braun P, Foldi M, Kisfaludy S, Szabo GY. Nature. 1956; 177:1133. [PubMed: 13334501]

44. a) Rehor A, Hubbell JA, Tirelli N. Langmuir. 2004; 21:411. [PubMed: 15620332] b) Thomas SN, van der Vlies AJ, O'Neil CP, Reddy ST, Yu SS, Giorgio TD, Swartz MA, Hubbell JA. Biomaterials. 2011; 32:2194. [PubMed: 21183216]

45. Saville B. Analyst. 1958; 83:670.

46. Hart TW. Tetrahedron Lett. 1985; 26:2013.

47. Michalski ML, Griffiths KG, Williams SA, Kaplan RM, Moorhead AR. PLoS Neglect Trop D. 2011; 5:e1261.
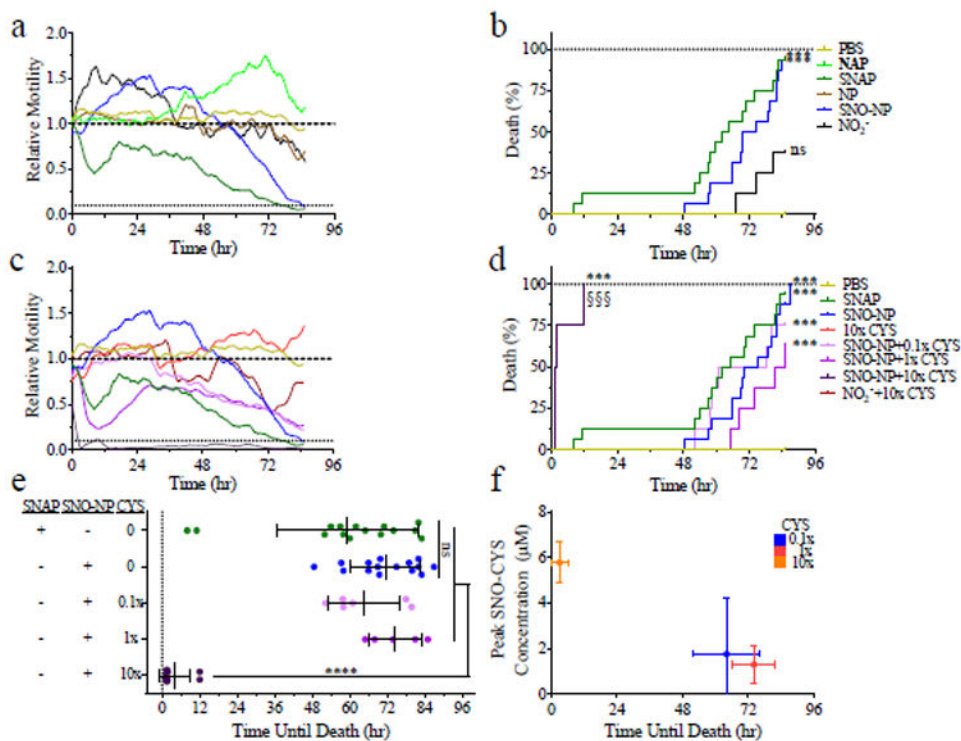
Figure 1.
Synthetic polymer nanoparticles are loaded with nitric oxide (NO) through the formation of physiological NO adducts, *S*-nitrosothiols (SNO), with NP thiols (SH). (a) NP synthesis and *S*-nitrosation scheme to create S-nitrosothiol (SNO) NP (SNO-NP). (b) Particle SH concentration is controlled by initiator concentration during emulsion polymerization synthesis. (c) NP diameter remains unchanged by SH concentration and NO loading. (d) SNO concentration and number per NP is proportional to NP SH concentration. NP-encapsulated NO is in the form of SNO as demonstrated by UV absorbance peaks at 340 (e) and is NP bound (f). (e) Arrow indicates increasing SNO-NP concentration. Data shown for a highest SNO-NP concentration of 5.6 mM with approximate 2 fold dilutions. Inset demonstrates calculation of molar extinction coefficient that was found to be 540 $M^{-1}cm^{-1}$. (g) Whereas nitrite (NO_2^-) remaining after S-nitrosation of SH-NP is rapidly dialyzed away, SNO signal by the Saville assay is retained.
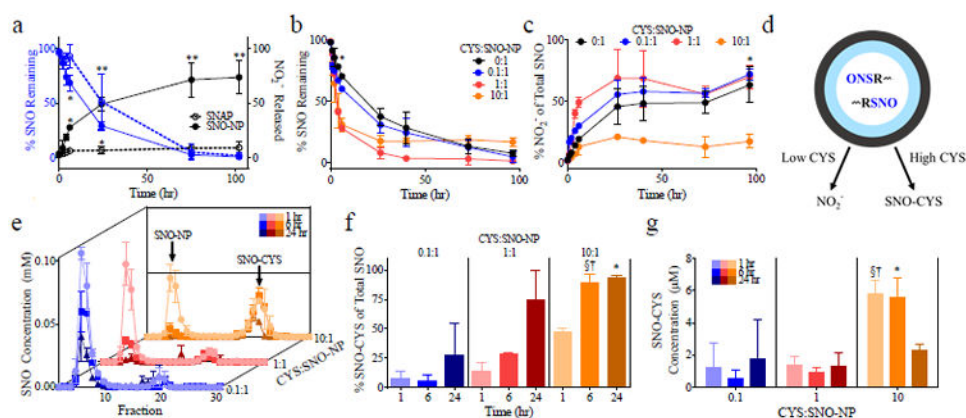
Figure 2.
SNO-NP mediate transnitrosation under high but not low concentrations of physiological thiol (SH) cysteine (CYS) in complete medium at 37°C. (a) Under conditions of no exogenously added CYS, decay of SNO from SNO-NP is comparable to that of low molecular weight NO donor, S-N-acetyl penicillamine (SNAP) but results in formation of nitrite (NO_2^-). (b-c) High (10:1) but not low (0:1, 0.1:1 and 1:10) ratios of CYS to SNO-NP result in long lived SNO species (b) and minimal SNO-NP release of NO_2^- (c). (d) Scheme of free thiol (CYS)-dependent NO release from SNO-NP to form NO_2^- or SNO-CYS via transnitrosation. Column chromatography fractionation of NP and CYS at various CYS:SNO-NP ratios (e) reveals increased formation of SNO-CYS with increasing co-incubation time and increasing CYS:SNO-NP ratio (f-g). (a-c) *p<0.05 and **p<0.01 by two-way ANOVA with matching and post-hoc Bonferroni tests. (f-g) *, §, † p<0.05 by two-way ANOVA with matching and post-hoc Bonferroni tests relative to 0.1:1 at 1460 min, 0.1:1 at 375 min, and 1:1 at 375 min, respectively. In all experiments, a SNO-NP concentration of 1 mM SNO was used.
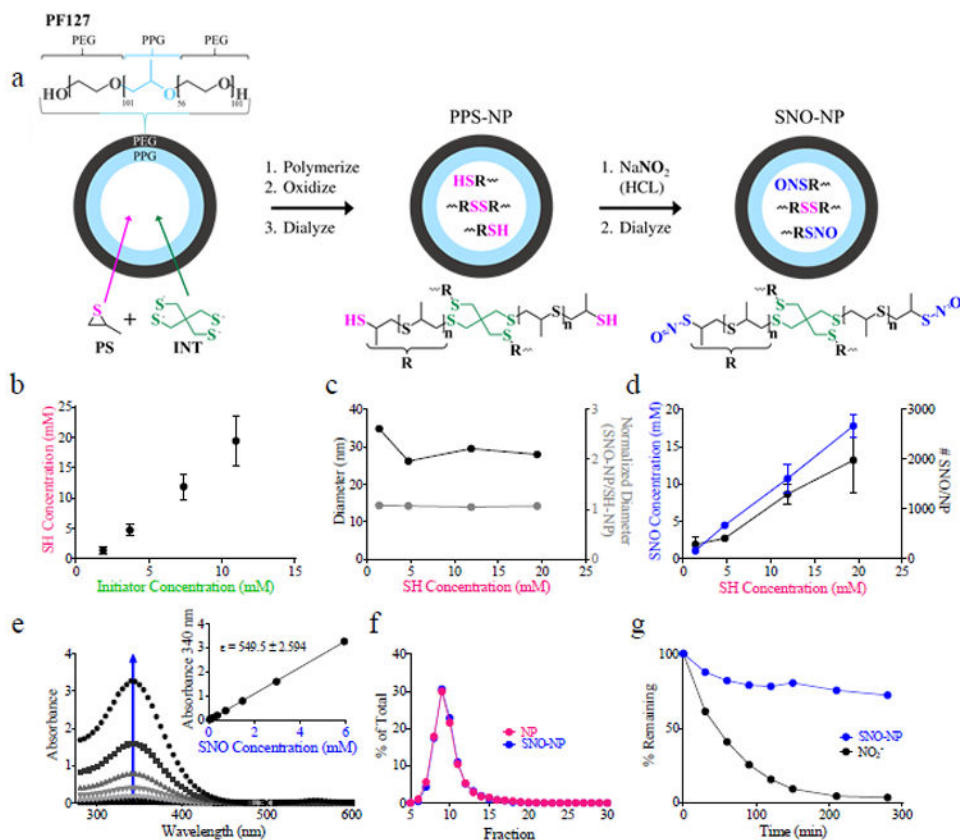
Figure 3.
SNO-NP-mediated killing of adult female B. malayi filarial worms is accelerated with increasing ratios of low molecular weight thiol cysteine (CYS) to SNO-NP. Worm motility (a) is reduced by NO donors SNO-NP and S-N-acetyl penicillamine (SNAP) and results in worm death at similar times (b). (c) Increasing ratio of CYS to SNO-NP accelerates SNO-NP-mediated reductions in worm motility. (d-e) Worm death induced by SNO-NP occurs more quickly at the highest ratios of CYS to SNO-NP relative to SNAP. Data in all panels from at least two independently run experiments. (a, c) Data represent the average motility of of n 8 worms. (b, d), *** and §§§ p<0.001 by Log-rank test. (e), *p<0.5 by one-way ANOVA with multiparameter comparison correction (Tukey's test). (f) Shortest time until worm death induced by SNO-NP corresponds to the ratio of CYS to SNO-NP that results in the highest observed levels of formed SNO-CYS concentrations. In all experiments, SNO-NP and SNAP concentrations of 1-2 mM SNO were used.